Chem Biol Drug Des 2012; **79:** 92–103

Research Article

doi: 10.1111/j.1747-0285.2011.01251.x

Cytotoxic Properties of Adamantyl Isothiocyanate and Potential *In vivo* Metabolite Adamantyl-*N*-Acetylcystein in Gynecological Cancer Cells

Thilo S. Lange[1,2,*], Timothy C. Horan[1], Kyu K. Kim[1], Ajay P. Singh[3], Nicholi Vorsa[3], Laurent Brard[4], Richard G. Moore[1] and Rakesh K. Singh[1,*]

[1]*Molecular Therapeutics Laboratory, Program in Women's Oncology, Department of Obstetrics and Gynecology, Women and Infants' Hospital, Alpert Medical School, Brown University, Providence, RI 02905, USA*

[2]*Department of Molecular Biology, Cell Biology, and Biochemistry, Brown University, Providence, RI 02912, USA*

[3]*Department of Plant Biology, Rutgers University, New Brunswick, NJ 08901, USA*

[4]*Division of Gynecologic Oncology, Department of Obstetrics and Gynecology, Southern Illinois University School of Medicine, Springfield, IL 62794, USA*

**Corresponding authors: Thilo S. Lange, thilo_lange@brown.edu; Rakesh K. Singh, rsingh@wihri.org*

This study determined the *in vitro* potential of novel compounds adamantyl-*N*-acetylcystein and adamantyl isothiocyanate to treat gynecological cancers. Adamantyl-*N*-acetylcystein is postulated to be an *in vivo* metabolite of adamantyl isothiocyanate as dietary isothiocyanates are converted to *N*-acetylcysteine-conjugates. A viability assay suggested that adamantyl isothiocyanate and adamantyl-*N*-acetylcystein are cytotoxic to cancer cells including gynecological cell lines. A NCI60 cancer cell assay revealed that growth-inhibition and cytotoxicity of adamantyl-*N*-acetylcystein were cell line, but not tissue type-specific. Cell cycle studies revealed that adamantyl-*N*-acetylcystein and adamantyl isothiocyanate arrest SKOV-3 ovarian cancer cells in G2/M phase. By TUNEL, immunoblotting, and viability studies employing caspase and p38 mitogen-activated protein kinase inhibitors, we proved that reduction in SKOV-3 viability is a consequence of DNA fragmentation and apoptosis. Cytotoxic action of adamantyl-*N*-acetylcystein in SKOV-3 and endometrial cancer (ECC-1, RL95-2, AN3CA, and KLE) cells required excess generation of reactive oxygen species which could be blocked by antioxidant co-treatment. Adamantyl-*N*-acetylcystein treatment led to modified expression or activation of apoptotic and oncogenic proteins such as JNK/SAPK, AKT, XIAP, and EGF-R for SKOV-3 and JNK/SAPK and ERK1/2 for ECC-1 cells. We suggest the further development of adamantyl-*N*-acetylcystein by sensitizing cells to the drug using signaling inhibitors or redox-modulating agents and by evaluating the drug efficacy in ovarian and endometrial *in-vivo* tumor models.

Key words: adamantyl-*N*-acetylcystein, apoptotic signaling, cytotoxicity, endometrial cancer, ovarian cancer, reactive oxygen species generation

Abbreviations: AC-AM, adamantyl-*N*-acetylcystein; FACS, fluorescent-activated cell sorting; ITC, isothiocyanate; ITC-AM, adamantyl isothiocyanate; MAPK, mitogen-activated protein kinase; ROS, reactive oxygen species.

Received 11 April 2011, revised 9 September 2011 and accepted for publication 27 September 2011

Epithelial ovarian cancer represents the most lethal and uterine endometrial cancer the most common gynecologic cancer. Ovarian cancer caused approximately 13 800 deaths, and 21 800 new cases were diagnosed in the year 2010 in the United States. Approximately 43 000 new cases of endometrial cancer are diagnosed each year in the United States with 7900 deaths occurring annually secondary to this malignancy.[a] Initial treatment for each of these cancers involves surgical staging to determine the extent of disease and need for adjuvant treatment. When systemic disease is identified as cytotoxic, chemotherapy plays an important role in the treatment of patients with advanced stage disease. Despite systemic chemotherapy, the majority of patients with ovarian cancer will experience a recurrence of their disease with median progression free survival of about 18 months and median overall survival of 38 months (1,2). Many of these patients with recurrent disease will ultimately develop platinum- and multidrug-resistant tumors. In contrast to ovarian cancer, the majority of patients with endometrial cancer will be diagnosed with early-stage disease and cured with surgery alone (3). However, for patients with advanced stage or recurrent endometrial cancer, adjuvant treatment with systemic chemotherapy is required. The current chemotherapeutic regimens for advanced stage or recurrent endometrial cancer can include, either alone or in combination, doxorubicin, platinum, and taxanes. The drug combination of cisplatin and doxorubicin in patients with systemic disease has a response rate of

up to 42% with a progression-free survival of 5.7 months as reported by Thigpen *et al.* (4). Similarly, the drug combination of paclitaxel and carboplatin yielded response rates of 78% in patient treated for primary disease with a median progression-free survival of 23 months (5). For each of these malignancies, chemoresistant tumors are problematic in the treatment and management of the patients. For these reasons, novel drugs are essential to improve the response rates and efficacies of current chemotherapeutic regimens.

Isothiocyanates (ITC) present as thioglucoside conjugates in cruciferous vegetables are a newly recognized class of potential antitumor agents and suppressors of multi-drug resistance in cancer (6). Phytochemical dietary ITC in the human body are converted to glutathione, cysteinylglycine, and mercapturic acid derivatives or *N*-acetylcysteine metabolites that can be disposed of through urinary excretion. For various ITC, as well as their *N*-acetylcysteine conjugates, antitumorigenic activity *in vivo* was shown (7–10). The objectives of this study were (i) to design an ITC derivative with improved antineoplastic features that (ii) displays preserved cytotoxic activity even after conversion into the *N*-acetylcysteine derivative and to (iii) treat gynecological tumors such as ovarian or endometrial cancer.

Naturally occurring ITC such as BITC, PEITC, and sulforaphane were shown to induce cell cycle arrest and apoptosis (11–13), to suppress angiogenesis with disruption of microtubule polymerization (14,15) and to inhibit the function of P-glycoproteins and other factors implicated in emergence of drug resistance (16,17). Antineoplastic effects of dietary *N*-acetylcysteine conjugates, for example, benzyl and phenethyl ITC, are based on similar mechanistic effects as their parent compounds, such as induction of apoptosis, cell cycle arrest, p53, matrix-metalloproteinase- and mitogen-activated-protein-kinase (MAPK) activation (18–20). In addition, synthetic ITC such as E-4IB, PHITC, 7Me-IEITC, or NB7M with increased *in vitro* potency as compared to various naturally occurring ITC have been developed. Cytotoxic mechanisms of these electrophilic organic compounds, characterized by a (R-N=C=S) functionality, include rapid induction of apoptosis, alteration of MAPK signaling, and cell cycle inhibitory effects in cancer cells including ovarian cancer cell lines (21–25). To date, no studies describing the biological effects of *N*-acetylcysteine conjugates or other potential metabolites of these synthetic ITC have been published. In this manuscript, we describe a *de novo* synthesis of ITC-based compounds with an adamantyl moiety, adamantyl-*N*-acetylcystein (AC-AM) and adamantyl isothiocyanate (ITC-AM), and their cytotoxic effects against a panel of cells from different tumor tissues. The polycyclic adamantyl scaffold (also termed adamantane) was originally discovered in petroleum in 1933 and launched a new chemistry field studying the properties of polyhedral organic compounds. Adamantyl, first synthesized in 1941 (26), has been used in medical applications since the early 1960s and was introduced to the clinic as amino-derivatives, e.g., as 'Amantadine' for the treatment of influenza and Parkinson's disease and as 'Memantine' to treat Alzheimer's disease (27; and refs therein). Adamantyl moieties have also been used to modify the pharmacokinetics of clinical drugs (e.g., by reducing cholinesterase hydrolysis) or to add steric features as for therapeutic AIDS drug zidovudine. To date, studies on the biological functions of compounds with an adamantyl scaffold are limited. It has been suggested that retinoid compounds substituted with adamantyl or adamantyl derivatives inhibit angiogenesis and the growth of cell lines derived from cancer tissues including leukemia, breast, lung, and prostate tumors and induce apoptosis (28–30). In this report, we examined the therapeutic potential of AC-AM to treat platinum-resistant ovarian cancer cells and steroid-responsive and non-responsive endometrial cancer cells by analyzing the generation of reactive oxygen species (ROS) and associated pro-apoptotic signaling and cytotoxicity.

Material and Methods

Synthesis of AC-AM, ITC-AM

Synthesis of ITC-AM

Adamantyl methyl amine was dissolved in ethyl acetate/H_2O (1:1) and stirred at 0–5 °C in the presence of sodium bicarbonate (20% w/v). To the reaction mixture, thiophosgene (1.25 eq) was added dropwise. The mixture was stirred at 0–5 °C for 4 h, and thin-layer chromatography indicated complete conversion. The reaction mixture was transferred to a separatory funnel, the organic layer collected, dried over anhydrous sodium sulfate, and concentrated under reduced pressure to afford a semisolid that solidified to afford off-white solid ITC-AM characterized by mass spectrometry, MS = 208 $(M^+H)^+$.

Synthesis of AC-AM

To the solution of ITC-AM dissolved in ethyl acetate/H_2O (1:1), commercially available *N*-acetyl cysteine (1.25 eq) was added, and the reaction mixture was stirred for 48 h at room temperature in the presence of sodium bicarbonate (20% w/v). The ethanol was removed under reduced pressure and the residue extracted with ethyl acetate (2 × 25 mL). The pH was lowered by dropwise addition of HCl (2N) until the solution turned milky white, and the reaction mixture was then extracted with ethyl acetate (3 × 25 mL). The organic layer was dried over anhydrous sodium sulfate and concentrated under reduced pressure to afford the cysteinyl derivative (AC-AM). Adamantyl-*N*-acetylcystein was characterized by mass spectroscopy and ^{1}H NMR ($CDCl_3$): 7.7571 (bs, 1H, NH), 7.61 (bs, 1H, NH), 4.64 (bs, 1H, CH), 3.94–3.83 (d, 2H, NCH_2), 3.52–3.47 (d, 2H, SCH_2), and 2.15–1.54 (m, 20H).

Adamantyl isothiocyanate and AC-AM were dissolved in DMSO (50 μM stock solution) and further diluted in media for tissue culture experiments. The final DMSO concentration in these assays was 0.08%. Controls were treated with the vehicle alone.

Cell culture

Human cell lines SKOV-3, (ovarian epithelial adenocarcinoma), HeLa (epithelial cervix adenocarcinoma), A-431 (epidermoid carcinoma), PC-3 (prostate adenocarcinoma), ECC-1, RL95-2, AN3CA, KLE (all endometrial adenocarcinoma; for specification, see Discussion section and http://www.atcc.org) were obtained from American Type Culture Collection (Manassas, VA, USA), and HUVEC (human umbilical vein endothelial cells) were obtained from Lonza Inc. (Allendale, NJ, USA). TCL-1 cell line (immortalized retroviral large T-antigen

transfected trophoblasts) was provided by Dr. S. Sharma (Woman & Infants Hospital, Providence, RI, USA) and the SMS-KCNR neuroblastoma cell line by Dr. Giselle Saulnier Sholler (University of Vermont, Burlington, VT, USA). All cells were seeded at 5×10^5/T75 cell culture flask (Corning, New York, NY, USA) and cultured to approximately 80% confluency according to the provider's recommendations in complete medium supplemented with 10% fetal bovine serum (Atlanta Biologicals, Lawrenceville, GA, USA), 100 U/mL penicillin, and 100 μg/mL streptomycin at 37 °C, 5% CO_2, in a humidified incubator. RL95-2 were grown in complete DMEM supplemented with 0.005 mg/mL insulin (SAFC Biosciences, Lenexa, KS, USA). For all assays, cells were collected by trypsinization (0.25% Trypsin-EDTA), washed in complete medium, and allowed to attach overnight before treatment as indicated in complete medium. Antioxidant ascorbic acid (Sigma-Aldrich, St. Lois, MO, USA) was added to some assays as indicated in the result section at the concentration of 500 μM to determine the effect of scavenging of radicals before and after drug treatment.

Cell viability assay

Viability of cell lines was determined by the CellTiter 96® AQueous One Solution Assay (Promega Corp, Madison, WI, USA), following the manufacturer's recommendations with suitable modifications (31). Briefly, cells were seeded into a 96-well microtiter plate at 1×10^4 cells/100 μL per well and treated in complete medium (DMSO) as indicated for 24 h. During the last 4 h of incubation, the MTS reagent was added at a 1:10 dilution to the medium. For assays with inhibitors (p38 MAPK: #559389; Calbiochem, La Jolla, CA, USA; Pan-caspase #FMK001, caspase-3 Z-DEVD-FMK and caspase-9 #Z-LEHD-FMK; R&D Systems, Minneapolis, MN, USA), the cells were preincubated with 40 μM inhibitor for 2 h prior to adding the drug. After the treatment period, absorbance was measured at 490 nm in an ELISA plate reader (Thermo Labsystems, Waltham, MA USA). Experiments were performed in triplicates; data are expressed as the mean of the triplicate determinations (X ± SD) of a representative experiment in percentage of absorbance by samples with untreated cells [=100%].

NCI 60 cancer cell line assay

Adamantyl-*N*-acetylcystein was screened through the National Cancer Institute (NCI) Developmental Therapeutics Program 60 human cancer cell line panel under the *in vitro* Cell Line screening Project. Briefly, cells (5000–40 000 cells/well depending on the cell line studied) were inoculated into 96-well microtiter plates in 100 μL complete RPMI1640 medium (5% FBS and 2 mM L-glutamine) and incubated 24 h prior to the addition of AC-AM. After the addition of the drug, the plates were incubated at 37 °C, 5% CO_2, 95% air, and 100% relative humidity for an additional 48 h. Upon the addition of 50 μL of cold TCA (10% TCA), the assay was terminated and incubated for 60 min at 4 °C to fix the cells. The supernatant was discarded, and the plates were washed five times with water and air-dried. Sulforhodamine B solution (100 μL) at 0.4% (v/v) in 1% acetic acid was added to each well and plates incubated for 10 min at room temperature. After staining, unbound dye was removed by washing five times with 1% acetic acid, and the plates were air-dried. Bound stain was subsequently solubilized with 10 mM trizma base, and the absorbance was read on an automated plate reader at a wavelength of 515 nm. Using absorbance measurements [time zero (Tz), control growth (C), and test growth in the presence of drug at the drug concentration (Ti)], the percentage growth was calculated. Percentage growth inhibition was calculated as: $[(Ti-Tz)/(C-Tz)] \times 100$ for concentrations for which $Ti \geq Tz$, $[(Ti-Tz)/Tz] \times 100$ for concentrations for which $Ti < Tz$.

Cell cycle analysis

Cell cycle analysis and quantification of apoptosis were carried out by flow cytometry. SKOV-3 (1.0×10^6) cells were seeded into 100-mm cell culture dishes and treated with 10 μM ITC-AM or AC-AM for 12, 18, or 32 h. At the end of the incubation period, cells were harvested and transferred into 15-mL polypropylene centrifuge tubes. After centrifugation ($250 \times g$, 5 min), the cells were fixed by adding the ice-cold 70% ethanol solution gradually. The cells were stained in the buffer containing propidium iodide (100 μg/mL), sodium citrate (1 mg/mL), and Triton-X-100 (3 μL/mL) for 30 min at 37 °C in the dark. Data were acquired on a BD FACSort flow cytometer using CellQuest software (BD Immunocytometry Systems, San Jose, CA, USA) and analyzed using ModFit LT software (Verity Software House Inc., Topsham, ME, USA). Ten thousand events were analyzed for each sample. The same gate was used on all samples, ensuring that the measurements were taken on a standardized cell population.

TUNEL assay

DNA fragmentation was detected using the DeadEnd™ Fluorometric TUNEL System assay (Promega), according to the manufacturer's recommendations. Cells (5×10^3/well) were plated into 96–well, flat-bottom plates (Corning Inc., Corning, NY, USA), treated with 10 μM AC-AM, and the assay was carried out as described previously (31). Fluorescence of apoptotic cells (green; labeling of DNA nicks by fluorescein-12-dUTP) and of chromatin (red; staining of chromatin with propidium iodide) was detected by fluorescence microscopy with an inverted microscope (Nikon Eclipse TE2000-E; Nikon Instruments Inc., Melville, NY, USA) and a 10× objective. Four randomly chosen microscopic fields were captured.

Western blot analysis

SKOV-3 cells (1.5×10^6) were seeded into 100-mm cell culture dishes and treated with 10 μM AC-AM for 6, 18, or 32 h. Preparation of cell lysates, PAGE, and immunoblotting was carried out as described previously (32) in Cell Extraction Buffer (Invitrogen, Carlsbad, CA, USA) supplemented with protease inhibitor cocktail and phenylmethylsulfonyl fluoride (Sigma-Aldrich), according to the manufacturers' recommendations. Samples (50 μg/sample) were separated using the Xcell SureLock™ mini-cell electrophoresis system (Invitrogen) on NuPAGE® 4–12% Tris–Bis Gel in NuPAGE® MES SDS running buffer, transferred onto a PVDF membrane, blocked with 5% non-fat dry milk in PBS-Tween, and probed against various primary antibodies (*against caspase-3 #9665, caspase 9 #9501, XIAP #2045, non-activated p38 #4631, and against phosphorylated EGFR #4407S, ERK1/2 #436, p38 # 92155, AKT #193H12, JNK/SAPK #46687 all from rabbit in a dilution of 1:1000, Cell Signaling Technologies, Danvers, MA, USA; cleaved PARP-1 #51-90000*

from mouse, 1:2000, BD Biosciences, San Jose, CA, USA; or beta-actin #sc-47778 from mouse, dilution 1:2000, HE4 #sc-1603 from goat, dilution 1:100, Santacruz Biotechnology, Santa Cruz, CA, USA). The bands were visualized using horseradish peroxidase-conjugated secondary antibody (Amersham-Pharmacia Biotech, Piscataway, NJ, USA), followed by enhanced chemiluminescence (Upstate, Waltham, MA, USA) and documented by autoradiography (F-Bx810 Film; Phenix, Hayward, CA, USA).

Detection of intracellular ROS

Detection of intracellular ROS after SKOV-3 treatment with AC-AM was measured by flow cytometry using carboxy-H2DCFDA dye (Invitrogen) as a probe. Carboxy-H2DCFDA is the acetylated form of a reduced fluorescein derivative that is cell permeable and non-fluorescent. Once the acetate groups are cleaved by intracellular esterase activities, this compound becomes charged and retained within the cell. In the presence of a cellular oxidant, the compound is oxidized and produces green-fluorescence that is detected by flow cytometry. This dye detects the following ROS: hydrogen peroxide (H_2O_2), hydroxyl radical ($HO^{\bullet}$), and peroxyl radical ($ROO^{\bullet}$). Cells (1.0×10^6) were seeded into 100-mm cell culture dishes and treated with 10 μM AC-AM for 6 or 16 h. Following the treatment with AC-AM, cells were incubated with 25 μM of carboxy-H2DCFDA for 30 min at 37 °C with 5% CO_2 in a humidified incubator, harvested, washed with 1×PBS, and suspended in PBS. Data were acquired on a BD FACSort flow cytometer using CellQuest software (BD Immunocytometry Systems) and analyzed using ModFit LT software (Verity Software House Inc.).

Results

Adamantyl isothiocyanate and AC-AM are cytotoxic to various human cancer cell lines including gynecological tumor cells

For the present study, we designed new ITC-based compounds with an adamantyl scaffold, AC-AM and ITC-AM (Figure 1A). Adamantyl is a diamondoid cycloalkane consisting of three cyclohexane rings with a scaffold which is both rigid and virtually stress free. Adamantyl moieties can be used either as a scaffold for development of therapeutic agents or as a modifier of pharmacokinetics (27; and refs. therein). Adamantyl isothiocyanate was generated in one step from commercially available adamantyl amine and characterized by mass spectrometry, MS = 208 $(M^+H)^+$. Adamantyl-*N*-acetylcystein was generated in two steps from ITC-AM and commercially available *N*-acetyl cysteine (Material and Methods, Figure 1A) in good yield (85%) and characterized by mass spectroscopy and ^{1}H NMR. [^{1}H NMR ($CDCl_3$) data: 7.7571 (bs, ^{1}H, NH), 7.61 (bs, 1H, NH), 4.64 (bs, 1H, CH), 3.94–3.83 (d, 2H, NCH_2), 3.52–3.47 (d, 2H, SCH2), and 2.15–1.54 (m, 20H)]. Adamantyl isothiocyanate and AC-AM were dissolved in DMSO to a 50 μM stock solution, which for tissue culture experiments was further diluted in media; controls were treated with vehicle alone (DMSO at a concentration of 0.08%). Phytochemical dietary ITC in the human body are converted to *N*-acetylcysteine conjugates, metabolites that can be disposed of through urinary excretion. The postulated *in vivo* conversion between ITC-AM and AC-AM is depicted (Figure 1B).

In an initial approach to analyze potential antineoplastic effects of ITC-AM and its derivative AC-AM, we performed a viability assay employing various platinum-resistant cancer cell lines, SKOV-3 (ovarian cancer) and ECC-1 (endometrial cancer) in comparison with HeLa (cervical), PC-3 (prostate), A-431 (epidermoid) cancer cells, SMS-KCNR (neuroblastoma), as well as control TCL-1 (immortalized trophoblasts) cells. The cells were treated for 24 h with various concentrations (0–40 μM) of the drugs and a colorimetric MTS assay performed in which the resulting optical density is directly proportional to the number of living cells. Both novel compounds, ITC-AM and AC-AM, displayed dose-dependent cytotoxicity (Figure 2). Adamantyl-*N*-acetylcystein possessed a higher potency than ITC-AM. All cancer cell lines responded to either drug at a concentration of ≥20 μM. The cytotoxicity depending on the cell line studied ranged from 13% to 63% for ITC-AM (Figure 2, left panel) and 39–80% for AC-AM (Figure 2, right panel). At a drug concentration of 10 μM, AC-AM reduced the viability of ECC-1, PC-3, and SMS-KCNR but not of SKOV-3, HeLa, or A-431 cells. Endothelial HUVEC cells did not respond to 10 μM drug treatment but when treated with 20 or 40 μM, AC-AM displayed high cytotoxicity (unpublished data). At a concentration of 40 μM, both adamantyl derivatives were highly effective toward all cancer cell lines studied. In contrast, the viability of TCL-1 control cells was not significantly affected even at drug concentrations of 40 μM (Figure 2). This assay suggested that, unlike for other ITC-based compounds, both the ITC derivative of adamantyl and the *N*-acetylcystein derivative AC-AM are detrimental to cell lines derived from cancer tissues including those from endometrial, ovarian, and cervical cancer tumors (ECC-1, SKOV-3, and HeLa cells lines, respectively). Adamantyl-*N*-acetylcystein displayed a higher potency when compared to ITC-AM.

AC-AM display differential effects on cancer cell lines derived from various tissues in a NCI60 growth assay

The effects of AC-AM on a broad panel of chemoresistant cancer cell lines of different tissue-types were determined by an NCI60 cancer cell-line growth screen. The concentration of the drug achieving 50% growth inhibition (GI50), total growth inhibition (TGI), and 50% cytotoxicity (LC50) was determined by the dose–response curves against the five different concentrations of the drug ranging from 10 nM to 100 μM (Figure 3). Potent inhibitory activities by AC-AM ($GI50 < 3 \times 10^{-6}$ M) were observed for all cell lines tested including 13 gynecological cancer cell lines (six isolated from ovarian tumors including SKOV-3 and seven lines from breast tumors). Remarkably strong growth inhibition ($GI50 < 5 \times 10^{-7}$ M) was observed in four of eight ovarian cancer cell lines, five of seven breast cancer cell lines, two of two prostate cancer cell lines, five of eight melanoma cell lines, two of eight renal cancer cell lines, four of six leukemia cell lines, three of nine non-small cell lung cancer cell lines, and six of seven colon cancer cell lines. It is interesting to note that AC-AM in leukemia cells, contrary to all other cancer cell types studied, predominantly displayed cytostatic but not cytotoxic effects. The LC50 for five of six leukemia cell lines is >100 μM and could not be measured in this study. For the other cell lines, the range of the LC50 is between 3.9 μM (LOX IMVI) and 69 μM (OVCAR-8) (Figure 3). In summary, the growth-inhibitory and cytotoxic drug effects were cell line-specific but not tissue type-specific

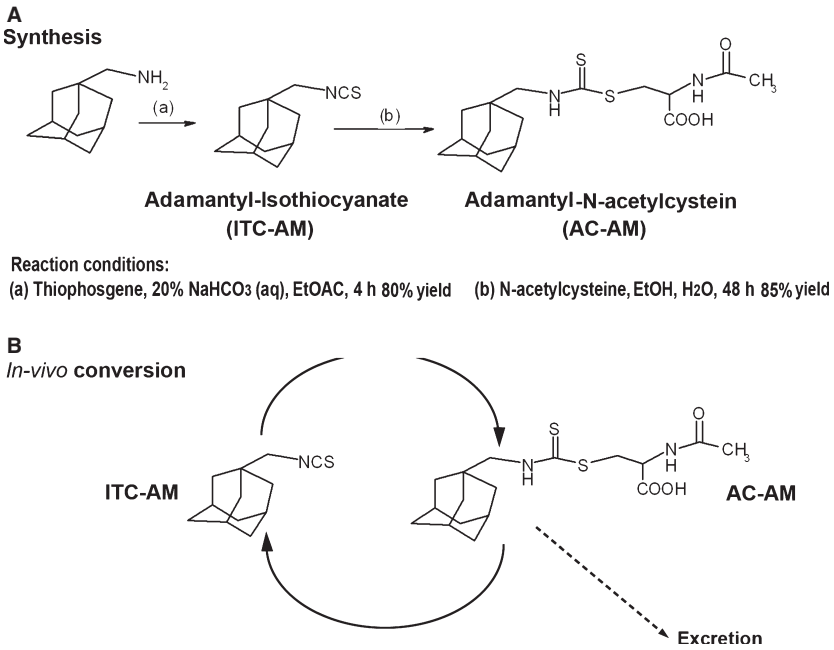

Figure 1: Drug design. (A) Synthesis of adamantyl-*N*-acetylcystein (AC-AM). Adamantyl-*N*-acetylcystein is generated from adamantyl and adamantyl isothiocyanate (AC-AM) as intermediate. (B) Postulated model of *in vivo* drug conversion. Phytochemical dietary isothiocyanate (ITC) in the human body are converted to *N*-acetylcysteine conjugates (N-AC). N-AC can be converted *in vivo* to ITC or are disposed of through urinary excretion. The postulated *in vivo* conversion between adamantyl isothiocyanate (ITC-AM) and AC-AM is depicted.

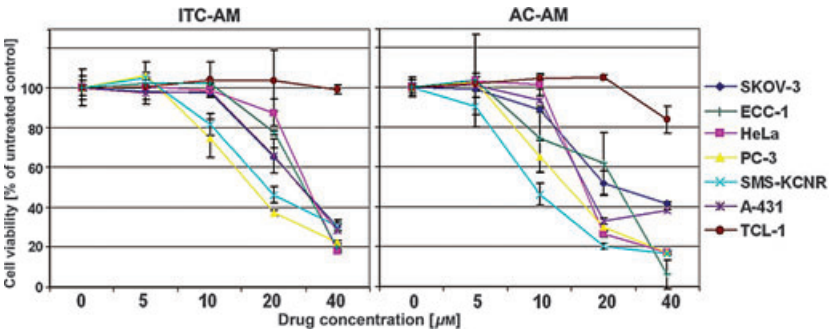

Figure 2: Comparative analysis of cytotoxic effects by adamantyl isothiocyanate (ITC-AM) and adamantyl-*N*-acetylcystein (AC-AM) in various human cancer cell lines. Human cell lines SKOV-3 (ovarian carcinoma), ECC-1 (endometrial carcinoma), HeLa (cervix carcinoma), SMS-KCNR (neuroblastoma), A-431 (epidermoid carcinoma), and TCL-1 (immortalized trophoblasts) were treated with various concentrations (5–40 μM) of ITC-AM or AC-AM for 24 h. The MTS viability assay was carried out as described (Material and Methods). Data are expressed as the mean of the triplicate determinations (X ± SD) of a representative experiment in % of absorbance by samples with untreated cells [=100%].

with the exception of the leukemia cell line. The viability assay performed by our laboratory in conjunction with the NCI60 screen suggests that AC-AM can potentially be developed to inhibit the growth of gynecological cancers and various other tumors.

Cell cycle arrest after treatment of SKOV-3 ovarian cancer cells with AC-AM in comparison with ITC-AM

We choose platinum-resistant SKOV-3 ovarian cancer cells to investigate by flow-cytometry whether AC-AM can cause disturbances of cell cycle progression. We compared the effects of AC-AM with those of ITC-AM to determine whether both adamantyl derivatives potentially affect the cell cycle to a similar degree and in the same phases. Cell cycle analysis of propidium iodide-stained SKOV-3 cells treated for 12, 28, or 32 h with 10 μM of either AC-AM or ITC-AM was carried out (Figure 4A). Both compounds caused a comparable increase in the count of apoptotic sub-diploidal/2n cells (sub-G0/G1, Figure 4B) in a time-dependent manner. With respect to cycling cells, both compounds caused a dose-dependent arrest of SKOV-3 in the G2/M phase and a correlated decrease in cells in G0/G1 phase. Within 12 and 18 h, cells were still capable of

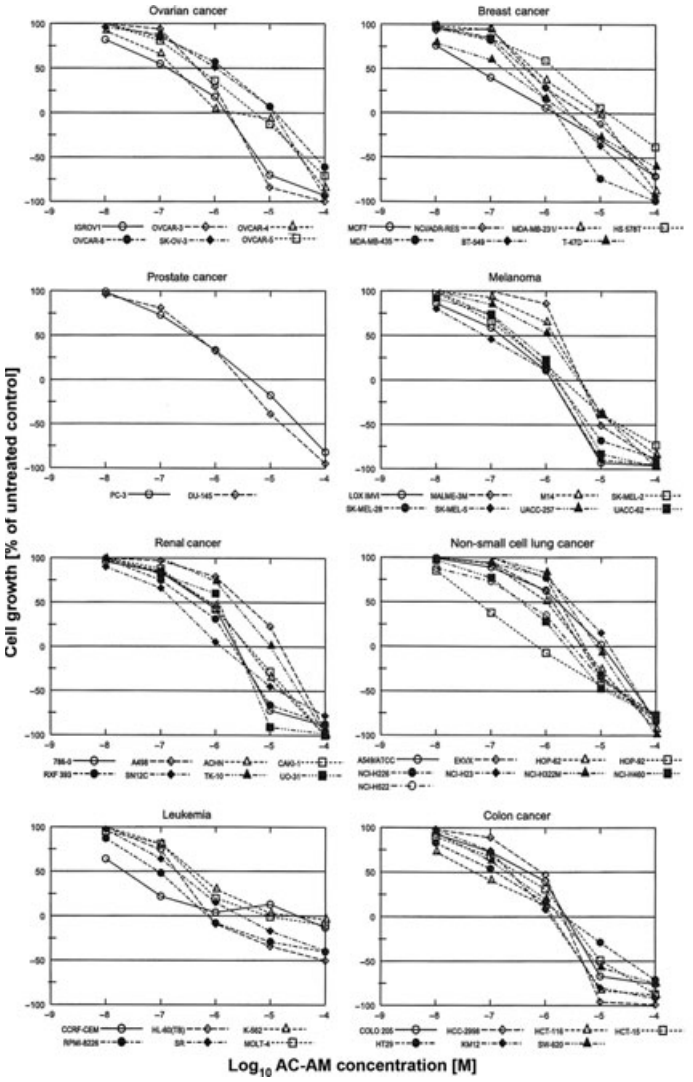

Cell line	Cell growth [%] Log10 AC-AM concentration [M] −8.0	−7.0	−6.0	−5.0	−4.0	GI50	TGI	LC50
Ovarian cancer								
IGROV1	82	55	18	−70	−93	1.33E-7	1.59E-6	5.89E-6
OVCAR-3	100	94	29	−84	−100	4.74E-7	1.81E-6	5.03E-6
OVCAR-4	92	66	4	−7	−85	1.80E-7	2.54E-6	3.56E-5
OVCAR-5	101	81	36	−13	−71	4.81E-7	5.32E-6	4.32E-5
OVCAR-8	101	85	57	7	−61	1.41E-6	1.26E-5	6.93E-5
SK-OV-3	96	88	51	7	−94	1.06E-6	1.16E-5	3.66E-5
Breast cancer								
MCF7	76	40	6	−30	−71	5.15E-8	1.45E-6	3.14E-5
NCI/ADR-RES	93	95	28	−12	−71	4.71E-7	4.96E-6	4.44E-5
MDA-MB-231/ATCC	98	94	37	−2	−88	5.98E-7	8.75E-6	3.63E-5
HS 578T	98	84	59	6	−38	1.46E-6	1.38E-5	> 1.00E-4
MDA-MB-435	96	82	16	−74	−99	3.04E-7	1.50E-6	5.44E-6
BT-549	97	85	29	−37	−94	4.24E-7	2.77E-6	1.68E-5
T-47D	79	60	16	−27	−60	1.66E-7	2.33E-6	4.91E-5
Prostate cancer								
PC-3	99	73	33	−18	−82	3.75E-7	4.47E-6	3.20E-5
DU-145	96	81	32	−39	−95	4.35E-7	2.85E-6	1.58E-5
Melanoma								
LOX IMVI	86	59	11	−93	−96	1.53E-7	1.29E-6	3.86E-6
MALME-3M	104	106	86	−51	−91	1.82E-6	4.22E-6	9.78E-6
M14	101	93	65	−38	−84	1.39E-6	4.28E-6	1.83E-5
SK-MEL-2	99	66	17	−38	−73	2.15E-7	2.06E-6	2.21E-5
SK-MEL-28	100	72	15	−68	−88	2.43E-7	1.52E-6	6.12E-6
SK-MEL-5	80	46	11	−90	−95	7.62E-8	1.27E-6	3.98E-6
UACC-257	100	85	53	−37	−98	1.08E-6	3.88E-6	1.64E-5
UACC-62	92	74	23	−83	−97	2.97E-7	1.64E-6	4.91E-6
Renal cancer								
786-0	96	84	43	−72	−89	6.68E-7	2.36E-6	6.40E-6
A498	105	97	79	23	−94	3.32E-6	1.58E-5	4.22E-5
ACHN	99	85	46	−35	−100	7.73E-7	3.66E-6	1.69E-5
CAKI-1	101	88	42	−28	−100	6.67E-7	4.01E-6	2.04E-5
RXF 393	99	75	31	−66	−87	3.76E-7	2.10E-6	6.90E-6
SN12C	90	66	5	−45	−78	1.84E-7	1.28E-6	1.43E-5
TK-10	110	107	74	1	−98	2.16E-6	1.03E-5	3.27E-5
UO-31	100	82	60	−91	−98	1.17E-6	2.50E-6	5.36E-6
Leukemia								
CCRF-CEM	64	22	4	13	−13	2.16E-8	3.26E-5	> 1.00E-4
HL-60(TB)	100	74	−9	−34	−50	1.95E-7	7.71E-7	9.70E-5
K-562	101	81	30	3	−4	4.06E-7	2.43E-5	> 1.00E-4
MOLT-4	95	81	20	−1	−10	3.20E-7	8.51E-6	> 1.00E-4
RPMI-8226	87	48	−8	−29	−40	8.85E-8	7.07E-7	> 1.00E-4
SR	97	64	15	−17	−39	1.91E-7	3.01E-6	> 1.00E-4
Non-small cell lung cancer								
A549/ATCC	99	89	63	2	−83	1.62E-6	1.07E-5	4.10E-5
EKVX	102	94	62	−35	−77	1.34E-6	4.36E-6	2.26E-5
HOP-62	110	93	51	−26	−93	1.02E-6	4.62E-6	2.30E-5
HOP-92	85	38	−7	−44	−77	5.55E-8	7.07E-7	1.47E-5
NCI-H226	109	109	77	−33	−85	1.77E-6	5.01E-6	2.11E-5
NCI-H23	101	94	78	15	−85	2.82E-6	1.42E-5	4.50E-5
NCI-H322M	101	107	83	−7	−99	2.30E-6	8.27E-6	2.93E-5
NCI-H460	97	77	28	−47	−79	3.60E-7	2.38E-6	1.27E-5
NCI-H522	88	73	35	−37	−80	3.95E-7	3.07E-6	2.03E-5
Colon cancer								
COLO 205	93	73	40	−67	−76	4.92E-7	2.36E-6	6.89E-6
HCC-2998	98	89	47	−96	−99	8.45E-7	2.13E-6	4.75E-6
HCT-116	73	41	13	−83	−88	5.21E-8	1.37E-6	4.54E-6
HCT-15	90	68	31	−49	−87	3.07E-7	2.45E-6	1.08E-5
HT29	83	54	16	−29	−71	1.28E-7	2.22E-6	3.11E-5
KM12	98	74	8	−80	−92	2.30E-7	1.23E-6	4.54E-6
SW-620	95	63	20	−57	−75	2.00E-7	1.83E-6	8.16E-6

Figure 3: Cell growth after adamantyl-*N*-acetylcystein (AC-AM) treatment in NCI60 cancer cell line screen. Cells were treated with AC-AM or vehicle and cell growth of the TCA fixed treated and untreated cells assessed (Material and Methods) after 48 h with sulforhodamine-B (SRB) solution and absorbance read at 515 nm.

progressing through S phase as indicated by a decreasing cell count. However, after 32 h of treatment, cells were arrested not only in G2/M (28.9% for AC-AM, 20.1% for ITC-AM, and 11.9% for controls) but also in S phase (33.3% for AC-AM, 32.9% for ITC-AM, and 22.6% for controls) while cell numbers in G0/G1 decreased (37.8% for AC-AM, 48.0% for ITC-AM, and 66.4% for controls) (Figure 4B). It is interesting to note that cell counts upon treatment for 12 or 18 h were similar for both compounds while after 32 h, AC-AM caused a significantly stronger arrest than ITC-AM.

DNA fragmentation and induction of apoptosis in SKOV-3 ovarian cancer cells after AC-AM treatment

As a first step to analyze the specific cell death-inducing mechanisms of AC-AM, we examined hallmark features of apoptosis in SKOV-3 cells. A TUNEL assay, a common method for detecting DNA fragmentation resulting from apoptotic signaling cascades, was carried out. SKOV-3 cells were treated for 24 h with AC-AM. Nuclei were counterstained with propidium iodide. TUNEL-positive nuclei were identified by yellow spots, resulting from an overlay of the image with apoptotic staining (FL-dUTP, green) and nuclear staining (Pi, red). As shown in Figure 5A, in contrast to untreated SKOV-3 cells, even at the low concentration of 10 μM of the drug, a significant number of cells displayed DNA fragmentation.

By immunoblotting, we analyzed the activation or de-activation of a variety of cellular markers such as caspases, PARP-1 or p38 MAPK, which play a key role in the morphological and biochemical changes associated with apoptosis. Adamantyl-*N*-acetylcystein treatment (10 μM) of SKOV-3 cells resulted in the activation/cleavage of initiator caspases-9, executioner caspase-3, and deactivation/cleavage of DNA repair factor PARP-1 starting at 6 h after addition of the drug and leveling off at 36 h of treatment (Figure 5B). Activation/

A

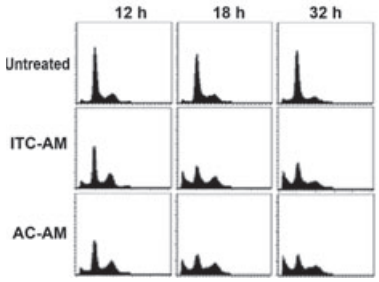

B

Drug	Treatment Time [h]	G0/G1 [%]	S [%]	G2/M [%]	Sub-G0/G1 Apoptosis [%]
Untreated	12	57.8	31.4	10.8	3.2
ITC-AM 10 μM		46.2	27.3	26.1	8.5
AC-AM 10 μM		45.2	27.7	27.2	7.7
Untreated	18	55.1	40.9	6.0	2.6
ITC-AM 10 μM		39.2	31.3	29.1	14.8
AC-AM 10 μM		37.4	31.8	30.9	13.3
Untreated	32	66.4	22.6	11.9	5.4
ITC-AM 10 μM		48.0	31.9	20.1	16.1
AC-AM 10 μM		37.8	33.3	28.9	16.3

Figure 4: Effect of adamantyl isothiocyanate (ITC-AM) or adamantyl-*N*-acetylcystein (AC-AM) on cell cycle progression in ovarian cancer cells. Cells were treated with 10 μM ITC-AM or AC-AM for 12, 18, or 32 h. Cell cycle analysis was carried out as described (Material and Methods). Data are presented as the relative fluorescence intensity of cell subpopulations in the two-dimensional FACS profile (panel A) and in % of cells in a given sub-population (panel B). Standardized gating was used for all samples. Ten thousand events were analyzed for each sample.

phosphorylation of pro-apoptotic p38 MAPK increased from the high basal level, which is common to ovarian cancer cells, within 18–36 h of AC-AM treatment. The proof that reduction in SKOV-3 viability by AC-AM is a direct consequence of the induction of apoptosis by these proteins is presented in Figure 5C. We employed a pan-case, caspase-3 or caspase-9 and a p38 MAPK inhibitor, which were added individually (40 μM) to the viability assay 2 h prior to and during treatment with AC-AM (0–40 μM). Cytotoxicity of 40 μM AC-AM was reduced by 76.9% following the addition of the pan-caspase inhibitor, by 62.4% following the addition of the caspase-3 inhibitor, by 51.7% following the addition of the caspase-9 inhibitor, and by 26.7% following the addition of the p38 MAPK inhibitor (Figure 5C). Accordingly, the activity of these pro-apoptotic factors each partially mediate AC-AM-induced apoptosis in ovarian cancer cells.

Generation of intracellular ROS by AC-AM in ovarian and endometrial cancer cells and block of cytotoxicity by antioxidant ascorbic acid

One potential strategy suggested to treat cancer is to generate an excess amount of ROS in tumor tissue to induce necrosis and/or apoptosis. We determined whether the treatment with AC-AM lead to excess generation of ROS in gynecological cancer cell lines. Various ROS species were detected via flow cytometry after carboxy-H2DCFDA staining, which emits green fluorescence in the presence of a cellular oxidant. As shown in Figure 6A, treatment with 10 μM AC-AM increased the ROS generation in both SKOV-3 ovarian cancer and ECC-1 endometrial cancer cells (shift in relative fluorescence intensity to right) as compared to untreated cells. This increase was achieved within 6 h of treatment for ECC-1 and 16 h for SKOV-3. To confirm that the generation of ROS by AC-AM is a predominant mechanism of cytotoxic action, we performed viability assays with SKOV-3 and ECC-1 cells, being treated (for 24 h) with antioxidant AA alone or in combination with 3 or 10 μM AC-AM. To verify the cytotoxic drug effect in endometrial cancer cell lines, we tested three other endometrial cancer cell lines (RL95-2, AN3CA, KLE) as cells from this tissue type, unlike for ovarian cancer, are not included in the NCI60 growth screen. As shown in Figure 6B, co-treatment with AA inhibited the cytotoxic effect of AC-AM in all cell lines tested. Cell viability upon treatment with AA alone (AA control) remained unchanged as compared to untreated cells. The cytotoxicity of AC-AM at both concentrations of the drug is higher for endometrial cancer cells as compared to SKOV-3 cells. Accordingly, the viability of ECC-1, RL95-2, AN3CA, and KLE, unlike for SKOV-3, was significantly restored by the antioxidant (Figure 6B). In summary, the elevation of ROS generation is a key mechanism of cytotoxic action by novel compound AC-AM.

AC-AM-induced cell signaling changes in ovarian and endometrial cancer cells

We analyzed the role of ROS in cellular signaling by treating SKOV-3 or ECC-1 cells with antioxidant AA alone or in combination with 10 μM AC-AM and subsequent Western blotting of cellular lysates. Antibodies against selected pro-survival, pro-apoptotic, and oncogenic signaling markers (XIAP, phosphorylated ERK1/2, JNK/SAPK, and AKT) were used. In addition, we included analysis of the activation of the epidermal growth factor (EGF) receptor and the expression of HE4 which is a biomarker for ovarian and endometrial cancer (33–35). ECC-1 and SKOV-3 cells displayed a differential expression or activation profile for these proteins after AC-AM treatment. SKOV-3 upon drug treatment downregulated expression of XIAP and phosphorylated AKT, upregulated activation of JNK/SAPK and EGF-R, while the activation of ERK1/2 remained similar to the untreated controls and HE4 could not be detected (Figure 6C). ECC-1, upon drug treatment, did not display changed levels of XIAP, HE4, and phosphorylated AKT or EGF-R but did demonstrate upregulated phosphorylation of JNK/SAPK and ERK1/2. Co-treatment with AC-AM and antioxidant AA did not block the described expression/activation changes observed after drug treatment. AA treatment alone did not affect marker expression with the exception of a slight de-activation of AKT in SKOV-3 and elevation of HE4 expression in ECC-1 cells (Figure 6C). In summary, ROS generation induced by AC-AM in ovarian SKOV-3 cancer cells and endometrial ECC-1 is a key mechanism of cytotoxic action. JNK/SAPK, AKT, and EGF-R in SKOV-3 cells and JNK/SAPK and ERK1/2 in ECC-1 cells were activated by AC-AM but not directly linked to ROS-mediated cell death.

Discussion

A low, 5-year, overall survival rate for women with advanced stage ovarian and endometrial cancer secondary to the development of

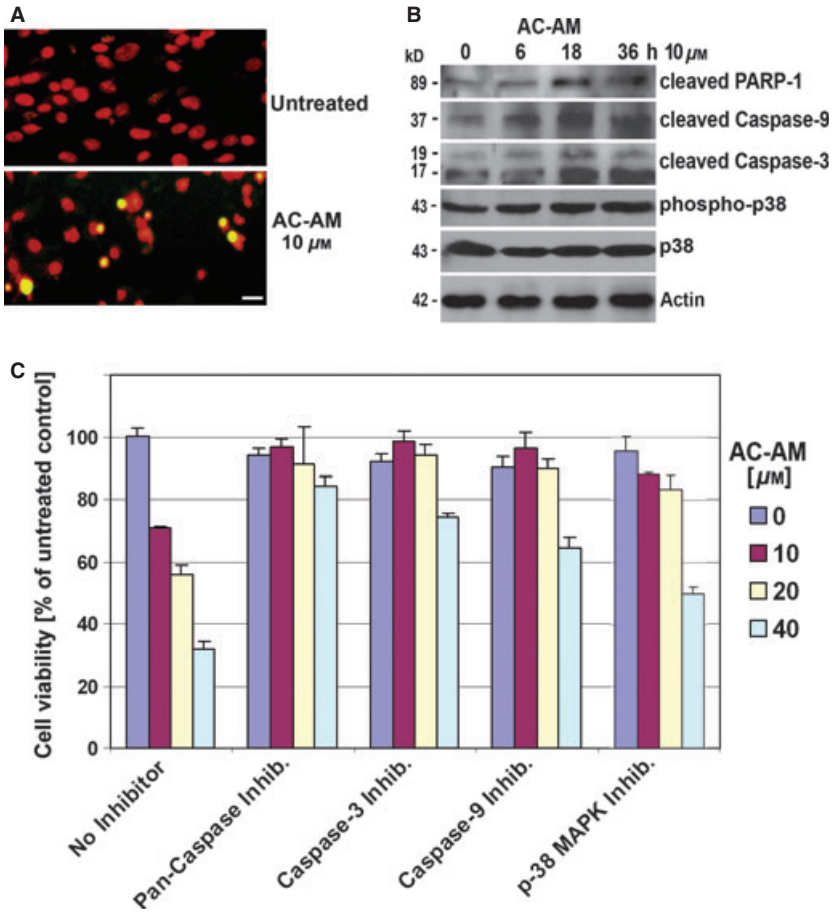

Figure 5: Induction of apoptosis in ovarian cancer cells after adamantyl-*N*-acetylcystein (AC-AM) treatment. (A) Analysis of DNA Fragmentation in a TUNEL Assay. SKOV-3 cells were treated with 10 μM AC-AM for 24 h. A TUNEL assay was carried out by co-staining with fluorescein-12-dUTP (labeling of DNA nicks in apoptotic cells) and of chromatin with propidium iodide (Material and Methods). During fluorescent microscopy, representative images were taken, apoptotic stain (green) and nuclear stain (red) overlaid. TUNEL-positive nuclei owing to DNA fragmentation appear as yellow areas. Bar = 10 μM. (B) Western blot analysis of pro-apoptotic marker activation. SKOV-3 cells were treated with 10 μM AC-AM for 24 h. PAGE and Western blot analysis of cell lysates were carried out. Inactivated/cleaved PARP-1 and activated/cleaved caspase-3 and caspase-9, p38 mitogen-activated protein kinase (MAPK) and activated/phosphorylated p38 MAPK were detected by immunoblotting as described in (Material and Methods). As an internal standard for equal loading (50 μg total cell protein/lane), blots were probed with an anti-β-actin antibody. (C) Effect of caspase and p38 inactivation on cell viability. SKOV-3 cells were preincubated with specific inhibitors (40 μM) against, caspase-3, caspase-9 and p38MAPK for 2 h and treated with AC-AM (0, 10, 20, or 40 μM) in the continued presence of the inhibitors (40 μM) for an additional 24 h. The MTS viability assay was carried out as described (Material and Methods). Data are expressed as the mean of the triplicate determinations (X ± SD) of a representative experiment in % of absorbance by samples with untreated cells [=100%].

multi-drug resistance of tumors to standard cytotoxic chemotherapeutic agents requires the development of new treatment options and anticancer drugs.[a] In the present study, we demonstrate the potential of both a synthetic isothiocyanate (ITC-AM) and its *N*-acetylcystein conjugate (AC-AM) to target ovarian and endometrial cancer cells; AC-AM is the postulated main metabolite in the human body. The resulting *in vivo* conversion between ITC-AM and AC-AM would amplify the cytotoxic effect. Acute and chronic toxicity studies in animal models will determine whether AC-AM or ITC-AM is the preferred compound of administration. For various ITC and their *N*-acetylcysteine conjugates, *in vivo* antitumorigenic activity was shown even though ITC can display a higher *in vivo* toxicity than their metabolites (8,9,36,37). The novel compounds designed for the present study carried an adamantyl moiety. Potential toxicities of compounds with an adamantyl group in general do not appear to be based on this moiety. Studies of potential anticancer drugs containing an adamantyl moiety are limited and were primarily based on retinoid compounds tested *in vitro* (28–30).

The present manuscript revealed that both ITC-AM and AC-AM diminished the viability of various cancer cell lines at drug concentrations ≥10 μM. In contrast, the viability of immortalized TCL-1 trophoblasts that possess a high metabolism and growth rate

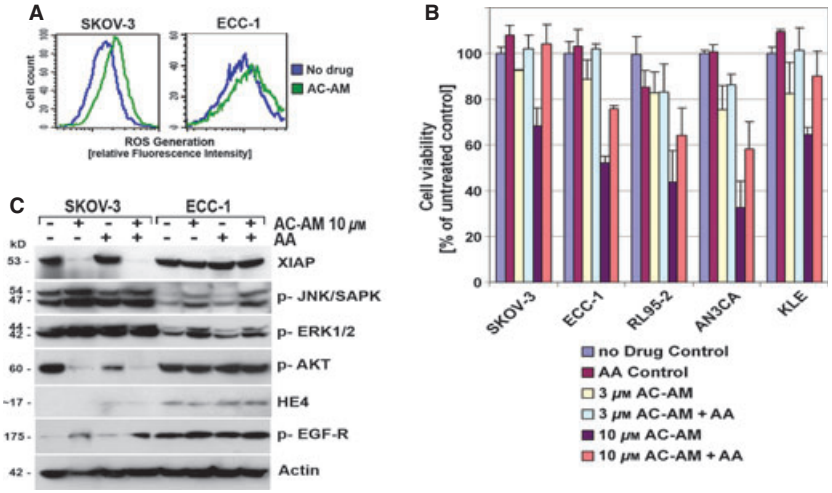

Figure 6: Adamantyl-*N*-acetylcystein (AC-AM)-induced reactive oxygen species (ROS) generation, cytotoxicity, and cell signaling in ovarian and endometrial cancer cells. (A) Generation of intracellular ROS. Reactive oxygen species generation in SKOV-3 (ovarian) or ECC-1 (endometrial) cancer cells was measured by flow cytometry (see Material and Methods). Cells were left untreated or treated with 10 μM AC-AM (6 h for ECC-1, 16 h for SKOV-3) and ROS generation compared. Data are presented as relative fluorescence intensity in a two-dimensional FACS profile. Standardized gating was used for all samples. (B) Ascorbic acid counteracts the cytotoxic effect of AC-AM. SKOV-3 (ovarian), ECC-1, RL95-2, AN3CA, KLE endometrial cancer cell lines were treated with AC-AM (3 or 10 μM) alone or in combination with ascorbic acid (AA, 500 μM) for 24 h. The MTS viability assay was carried out as described (Material and Methods). Experiments were performed in triplicates; data of a representative experiment are expressed as the mean of triplicate determinations (X ± SD) in % cell viability of samples with untreated cells [=100%]. (C) Expression of apoptotic and pro-survival markers after AC-AM treatment with or without ROS inhibition. SKOV-3 or ECC-1 cells were treated with 10 μM AC-AM in the absence or presence of ascorbic acid (AA, 500 μM) for 6 or 24 h. Analysis of the expression of proteins in cell lysates was carried out by PAGE and Western blot analysis with primary antibodies against phosphorylated pro-apoptotic JNK/SAPK, against pro-survival markers XIAP, phosphorylated Erk1/2 and AKT, against tumor marker HE4 and the phosphorylated epidermal growth factor (EGF) receptor. As an internal standard for equal loading, the blots were probed with an anti-β-actin antibody.

similar to most cancer cells and served as controls was not significantly affected even at drug concentrations of 40 μM. Broader effects of AC-AM on chemoresistant cancer cell lines of different tissue-types were determined by a NCI60 growth screen, which revealed that the growth-inhibitory and cytotoxic drug effects were cell line-specific but not tissue type-specific with the exception of leukemia cells. To test the selective cytotoxic potential of AC-AM in ovarian cancer cells, we chose the SKOV-3 cell line that is multi-drug-resistant (including cisplatin and adriamycin; see ATCC, Manassas, VA, USA; http://www.atcc.org) alongside ovarian cancer cell lines IGROV1, OVCAR-3, OVCAR-4, OVCAR-5, and OVCAR-8 present in the NCI60 screen. To examine the response of endometrial cancer cells to AC-AM, we chose four cell lines (ECC-1, RL95-2, AN3CA, KLE; http://www.atcc.org) cells from this tissue type that are not included in the NCI60 growth screen. Both ECC-1 and RL95-2 cell lines are well differentiated, steroid responsive, and tumorigenic. In contrast, AN3CA and KLE are poorly differentiated, steroid receptor defective, and tumorigenic. Adamantyl-*N*-acetylcystein was cytotoxic to each of these ovarian and endometrial cancer cell lines at a concentration of 10 μM and is a candidate drug to treat platinum-resistant ovarian tumors and endometrial tumors with various differentiation and or hormone receptor status.

The NCI60 study revealed that AC-AM inhibited the growth of multiple gynecological cancer cells at sub-cytotoxic concentrations with a GI50 between 52 nM and 1.5 μM for breast cancer cell lines and a GI50 between 133 nM and 1.4 μM for ovarian cancer cell lines. We choose platinum-resistant SKOV-3 ovarian cancer cells to explore the effects of AC-AM on cell cycle progression. Comparison of the effects of AC-AM with those of ITC-AM determined that both adamantyl derivatives affected the same phases of the cell cycle causing a dose-dependent arrest in G2/M phase and after an extended treatment (32 h) an additional arrest in S phase. In cancer cells, regulators of the cell cycle machinery are frequently altered, and transformed cells can be more sensitive to cyclin-dependent kinase inhibition (38–40). In future studies, we will analyze the role of AC-AM on specific cell cycle regulators including replication start and replication progression signals of S phase (41,42) in synchronized ovarian cancer, endometrial cancer, and non-transformed cell cultures. Targeting such checkpoints has been suggested as an alternative or supplemental approach to anticancer therapies (43,44).

Adamantyl-*N*-acetylcystein-induced cell death is mediated by a variety of pro-apoptotic factors including caspases, Mitogen-activated protein kinases, and in SKOV-3 cells can be partially prevented by the use of inhibitors against these proteins. P38 MAPK appears to play a significant role in the regulation of ovarian cancer by differential and competing effects. Previously, inactivation of p38 function (DN-p38 mutation in SKOV-3 and CaOV-3 by transient transfection) was shown to inhibit EGF-dependent ovarian cancer cell invasiveness (45), and p38 upregulation has been correlated with increased tumorigenesis in an ovarian cancer xenograft (46). In contrast, p38

activation is generally a pro-apoptotic trigger in ovarian cancer cells and is a key determinant for drug (platinum compound CDDP)-induced apoptosis (47). The use of p38 inhibitors *in vitro* can remarkably suppress the cytotoxicity of a variety of ITC-based drugs (21–23) as shown here for of AC-AM. Accordingly, we suggest future studies on the biochemical effect of AC-AM in ovarian cancer cells to include analysis of p38 signaling and related pathways such as EGF signaling (48). This cytokine constitutes a principal growth-promoting signal not only in ovarian cancer but also in endometrial cancer (48,49). However, contrary to the effect in ovarian cancer SKOV-3 cells, we did not observe a significant upregulation of the phosphorylation of the EGF-R in endometrial cancer cells.

As shown in the present report, cell death of ovarian cancer and endometrial cancer cells *in vitro* in response to treatment with AC-AM is linked to excess generation of ROS. Reactive oxygen species have been implicated in cancer initiation and progression. Cancer cells, presumably through mitochondria dysfunction and increased metabolism, generate a relatively high level of ROS (50,51). Upregulation of cellular ROS, such as shown here after treatment with AC-AM, has been suggested as a strategy to selectively target cancer cells over normal cells (52,53). Potentially, AC-AM may exert synergistic effects when combined with other agents thought to modulate the antioxidant functions of cancer cells, for example 2-methoxyestradiol (SOD inhibitor), tetrathiomolybdate, or ATN-224 (copper-depletion agents to target Cu/Zn SOD) and drugs leading to glutathione depletion such as buthionine-sulfoximine. Interestingly, ovarian SKOV-3 and endometrial ECC-1 cancer cells upon AC-AM displayed a differential expression or activation profile of pro-survival, pro-apoptotic, and oncogenic signaling markers. In ovarian cancer cells, a modulated activity of JNK/SAPK, AKT, and EGF-R was noted, whereas in endometrial cancer cells, JNK/SAPK and ERK1/2, but not AKT or EGF-R activity, was changed upon drug treatment. These changes were still observed after treatment with an antioxidant which, however, could partially block AC-AM-induced and ROS-mediated cell death. This observation is different than the findings by our laboratory to other drugs (e.g., organometallic compound iron(III)-salophene; ITC derivative ABITC) where ROS generation was the primary mechanism of cytotoxic action in neuroblastoma and endometrial cancer cells and strong activation of p38 and JNK could completely be abolished by cellular co-treatment with exogenous antioxidants (54,55). Similarly, recent studies suggested that the drug-induced activation of MAPK including JNK/SAPK and cancer cell apoptosis can be directly ROS dependent (56,57). Depending on the parameters (such as cell or drug type, drug concentration, or kinetics of treatment), pro-apoptotic signaling may be a direct consequence of increased ROS generation or depend on additional drug-induced mechanisms. In the case of AC-AM when applied at concentrations below the IC_{50} (e.g., 10 μM), elevated ROS generation reduced cell viability but did not directly correlate with the observed induced pro-apoptotic or diminished pro-survival signaling.

Conclusion

Findings in the present manuscript suggest that AC-AM can be developed for the treatment of various gynecological cancers and encourage future studies to determine the chemotherapeutic effect of this compound in animal tumor models. *In vivo* conversion between *N*-acetylcystein derivative AC-AM and isothiocyanate ITC-AM is suggested to amplify the cytotoxic effect of this newly designed compound. We propose to refine the ROS-mediated efficacy of AC-AM through structure modifications or by sensitizing target cells to the drug using inhibitors of pro-survival or growth factor (e.g., EGF)-signaling or redox-modulating agents.

Acknowledgments

RGM is partially supported by NCI Grant #1 RO1 CA136491-01 and Grants from Swim Across America. RKS is partially supported by Grants from Swim Across America.

References

1. McGuire W.P., Hoskins W.J., Brady M.F., Kucera P.R., Partridge E.E., Look K.Y., Clarke-Pearson D.L., Davidson M. (1996) Cyclophosphamide and cisplatin compared with paclitaxel and cisplatin in patients with stage III and stage IV ovarian cancer. N Engl J Med;334:1–6.
2. International Collaborative Ovarian Neoplasm Group (2002) Paclitaxel plus carboplatin versus standard chemotherapy with either single-agent carboplatin or cyclophosphamide, doxorubicin, and cisplatin in women with ovarian cancer: the ICON3 randomised trial. Lancet;360:505–515.
3. Creasman W.T., Morrow C.P., Bundy B.N., Homesley H.D., Graham J.E., Heller P.B. (1987) Surgical pathologic spread patterns of endometrial cancer. A gynecologic Oncology Group Study. Cancer;60:2035–2041.
4. Thigpen J.T., Brady M.F., Homesley H.D., Malfetano J., DuBeshter B., Burger R.A., Liao S. (2004) Phase III trial of doxorubicin with or without cisplatin in advanced endometrial carcinoma: a gynecologic oncology group study. J Clin Oncol;22:3902–3908.
5. Hoskins P.J., Swenerton K.D., Pike J.A., Wong F., Lim P., Acquino-Parsons C., Lee N. (2001) Paclitaxel and carboplatin, alone or with irradiation, in advanced or recurrent endometrial cancer: a phase II study. J Clin Oncol;19:4048–4053.
6. Hecht S.S. (2004) Chemoprevention by isothiocyanates. In: Kelloff G., Hawk E.T., Sigman C.C., editors. Promising Cancer Chemopreventive Agents, Vol 1: Cancer Chemopreventive Agents. Totowa, NJ: Humana Press; p. 21–35.
7. Conaway C.C., Wang C.X., Pittman B., Yang Y.M., Schwartz J.E., Tian D., McIntee E.J., Hecht S.S., Chung F.L. (2005) Phenethyl isothiocyanate and sulforaphane and their N-acetylcysteine conjugates inhibit malignant progression of lung adenomas induced by tobacco carcinogens in A/J mice. Cancer Res;65:8548–8557.
8. Conaway C.C., Yang Y., Lunk F.C. (2002) Isothiocynates as chemopreventive agents: their biological activities and metabolism in rodents and humans. Curr Drug Metab;3:233–255.
9. Tang L., Li G., Song L., Zhang Y. (2006) The principal urinary metabolites of dietary isothiocyanates, N-acetylcysteine conjugates, elicit the same anti-proliferative response as their parent compounds in human bladder cancer cells. Anticancer Drugs;17:297–305.

10. Chung F.L., Conaway C.C., Rao C.V., Reddy B.S. (2002) Chemoprevention of colonic aberrant crypt foci in Fischer rats by sulforaphane and phenethyl isothiocyanate. Carcinogenesis;21:2287–2291.
11. Kalkunte S., Swamy N., Dizon D.S., Singh R., Granai C.O., Brard L. (2006) Phenethyl isothiocyanate (PEITC) inhibits growth of ovarian cancer cells by inducing apoptosis: role of caspase and MAPK activation. Gynecol Oncol;103:261–270.
12. Kalkunte S., Swamy N., Dizon D.S., Granai C.O., Brard L. (2006) Benzyl Isothiocyanate (BITC) induces apoptosis in ovarian carcinoma. J Exp Ther Oncol;5:287–300.
13. Singh S.V., Herman-Antosiewicz A., Singh A.V., Lew K.L., Srivastava S.K., Kamath R., Brown K.D., Zhang L., Baskaran R. (2004) Sulforaphane-induced G2/M phase cell-cycle arrest involves checkpoint kinase 2-mediated phosphorylation of cell division cycle. J Biol Chem;279:25813–25822.
14. Jackson S.J., Singletary K.W., Venema R.C. (2007) Sulforaphane suppresses angiogenesis and disrupts endothelial mitotic progression and microtubule polymerization. Vascul Pharmacol;46:77–84.
15. Xiao D., Singh S.V. (2007) Phenethyl isothiocyanate inhibits angiogenesis in vitro and ex vivo. Cancer Res;67:2239–2246.
16. Barecki R.M., Wang E.J., Johnson W.W. (2003) Quantitative evaluation of isothiocyanates as substrates and inhibitors of P-glycoprotein. J Pharm Pharmacol;55:1251–1257.
17. Tseng E., Kamath A., Morris M.E. (2002) Effect of organic isothiocyanates on the P-glycoprotein- and MRP1-mediated transport of daunomycin and vinblastine. Pharm Res;19:1509–1515.
18. Yang Y.M., Conaway C.C., Chiao J.W., Wang C.X., Amin S., Whysner J., Dai W., Reinhardt J., Chung F.L. (2002) Inhibition of benzo(a)pyrene-induced lung tumorigenesis in A/J mice by dietary N-acetylcysteine conjugates of benzyl and phenethyl isothiocyanates during the postinitiation phase is associated with activation of mitogen-activated protein kinases and p53 activity and induction of apoptosis. Cancer Res;62:2–7.
19. Chiao J.W., Wu H., Ramaswamy G., Conaway C.C., Chung F.L., Wang L., Liu D. (2004) Ingestion of an isothiocyanate metabolite from cruciferous vegetables inhibits growth of human prostate cancer cell xenografts by apoptosis and cell cycle arrest. Carcinogenesis;25:1403–1408.
20. Hwang E.S., Lee H.J. (2006) Allyl isothiocyanate and its N-acetylcysteine conjugate suppress metastasis via inhibition of invasion, migration, and matrix metalloproteinase-2/-9 activities in SK-Hep 1 human hepatoma cells. Exp Biol Med;231:421–430.
21. Singh R.K., Lange T.S., Kim K., Zou Y., Lieb C., Sholler G.L., Brard L. (2007) Effect of indole ethyl isothiocyanates on proliferation, apoptosis and MAPK signaling in neuroblastoma cell lines. Bioorg Med Chem Lett;17:5846–5852.
22. Brard L., Singh R.K., Kim K.K., Lange T.S., Sholler G.S. (2009) Induction of cytotoxicity, apoptosis and cell-cycle arrest by 1-t-butyl carbamoyl, 7-methyl-indole-3-ethyl isothiocyanate (NB7M) in nervous system cancer cells. Drug Des Devel Ther;2:61–69.
23. Singh R.K., Lange T.S., Kim K.K., Singh A.P., Vorsa N., Brard L. (2008) Isothiocyanate NB7M causes selective cytotoxicity, pro-apoptotic signaling and cell-cycle regression in ovarian cancer cells. Br J Cancer;99:1823–1831.
24. Singh R.K., Lange T.S., Shaw S., Kim K.K., Brard L. (2008) A novel Indole Ethyl Isothiocyanate (7Me-IEITC) with anti-proliferative and pro-apoptotic effects on platinum-resistant ovarian cancer cells. Gyn Onc;109:240–249.
25. Bodo J., Hunakova L., Kvasnicka P., Jakubikova J., Duraj J., Kasparkova J., Sedlak J. (2006) Sensitisation for cisplatin-induced apoptosis by isothiocyanate E-4IB leads to signalling pathways alterations. Br J Cancer;95:1348–1353.
26. Prelog V., Seiwerth R. (1941) Über die Synthese des Adamantans. Berichte;74:1644–1648.
27. Van der Schyf C.J., Geldenhuys W.J. (2009) Polycyclic compounds: ideal drug scaffolds for the design of multiple mechanism drugs? Neurotherapeutics;6:175–186.
28. Pfahl M. (2004) Apoptosis inducing adamantyl derivatives and their usage as anti-cancer agents, especially for cervical cancers and dysplasias. United States Patent 6825226
29. Farhana L., Dawson M.I., Huang Y., Zhang Y., Rishi A.K., Reddy K.B., Freeman R.S., Fontana J.A. (2004) Apoptosis signaling by the novel compound 3-Cl-AHPC involves increased EGFR proteolysis and accompanying decreased phosphatidylinositol 3-kinase and AKT kinase activities. Oncogene;23:1874–1884.
30. Dawson M.I., Xia Z., Liu G., Ye M., Fontana J.A., Farhana L., Patel B.B. *et al.* (2007) An adamantyl-substituted retinoid-derived molecule that inhibits cancer cell growth and angiogenesis by inducing apoptosis and binds to small heterodimer partner nuclear receptor: effects of modifying its carboxylate group on apoptosis, proliferation, and protein-tyrosine phosphatase activity. J Med Chem;50:2622–2639.
31. Lange T.S., Kim K.K., Singh R.K., Strongin R.M., McCourt C.K., Brard L. (2008) Iron(III)-salophene: an metallo-organic compound with selective cytotoxic and anti-proliferative properties in platinum-resistant ovarian cancer cells. PLoS ONE;3:e2303.
32. Lange T.S., Singh R.K., Kim K.K., Zou Y., Kalkunte S.S., Sholler G.L., Swamy N., Brard L. (2007) Anti-proliferative and pro-apoptotic properties of 3-Bromoacetoxy Calcidiol (B3CD) in high-risk neuroblastoma. Chem Biol Drug Des;70:302–310.
33. Li J., Dowdy S., Tipton T., Podratz K., Lu W.G., Xie X., Jiang S.W. (2009) HE4 as a biomarker for ovarian and endometrial cancer management. Expert Rev Mol Diagn;9:555–566.
34. Moore R.G., McMeekin D.S., Brown A.K., DiSilvestro P., Miller M.C., Allard W.J., Gajewski W., Kurman R., Bast R.C. Jr, Skates S.J. (2009) A novel multiple marker bioassay utilizing HE4 and CA125 for the prediction of ovarian cancer in patients with a pelvic mass. Gynecol Oncol;112:40–46.
35. Moore R.G., Brown A.K., Miller M.C., Badgwell D., Lu Z., Allard W.J., Granai C.O., Bast R.C. Jr, Lu K. (2008) Utility of a novel serum tumor biomarker HE4 in patients with endometrioid adenocarcinoma of the uterus. Gynecol Oncol;110:196–201.
36. Witschi H., Espiritu I., Yu M., Willits N.H. (1998) The effects of phenethyl isothiocyanate, N-acetylcysteine and green tea on tobacco smoke-induced lung tumors in strain A/J mice. Carcinogenesis;19:1789–1794.
37. Masutomi N., Toyoda K., Shibutani M., Niho N., Uneyama C., Takahashi N., Hirose M. (2001) Toxic effects of benzyl and allyl isothiocyanates and benzyl-isoform specific metabolites in the urinary bladder after a single intravesical application to rats. Toxicol Pathol;29:617–622.
38. Hartwell L.H., Kastan M.B. (1994) Cell-cycle control and cancer. Science;266:1821–1828.

39. Gladden A.B., Diehl J.A. (2003) Cell-cycle progression without cyclin E/CDK2: breaking down the walls of dogma. Cancer Cell;4:160–162.
40. Aggarwal P., Lessie M.D., Lin D.I., Pontano L., Gladden A.B., Nuskey B., Goradia A., Wasik M.A., Klein-Szanto A.J., Rustgi A.K., Bassing C.H., Diehl J.A. (2007) Nuclear accumulation of cyclin D1 during S phase inhibits Cul4-dependent Cdt1 proteolysis and triggers p53-dependent DNA rereplication. Genes Dev;21:2908–2922.
41. Pines J. (1999) Four-dimensional control of the cell-cycle. Nat Cell Biol;1:73–79.
42. Stillman B. (1996) Cell-cycle control of DNA replication. Science;274:1659–1664.
43. Shapiro G.I., Harper J.W. (1999) Anticancer drug targets: cell-cycle and checkpoint control. J Clin Invest;104:1645–1653.
44. Mazumder S., DuPree E.L., Almasan A. (2004) A dual role of cyclin E in cell proliferation and apoptosis may provide a target for cancer therapy. Curr Cancer Drug Targets;4:65–75.
45. Zhou H.Y., Pon Y.L., Wong A.S. (2007) Synergistic effects of epidermal growth factor and hepatocyte growth factor on human ovarian cancer cell invasion and migration: role of extracellular signal-regulated kinase 1/2 and p38 mitogen-activated protein kinase. Endocrinology;148:5195–5208.
46. Chauhan S.C., Vannatta K., Ebeling M.C., Vinayek N., Watanabe A., Pandey K.K., Bell M.C., Koch M.D., Aburatani H., Lio Y., Jaggi M. (2009) Expression and functions of transmembrane mucin MUC13 in ovarian cancer. Cancer Res;69:765–774.
47. Mansouri A., Ridgway L.D., Korapati A.L., Zhang Q., Tian L., Wang Y., Siddik Z.H., Mills G.B., Claret F.X. (2003) Sustained activation of JNK/p38 MAPK pathways in response to cisplatin leads to Fas ligand induction and cell death in ovarian carcinoma cells. J Biol Chem;278:19245–19256.
48. Benedetti V., Perego P., Luca Beretta G., Corna E., Tinelli S., Righetti S.C., Leone R., Apostoli P., Lanzi C., Zunino F. (2008) Modulation of survival pathways in ovarian carcinoma cell lines resistant to platinum compounds. Mol Cancer Ther;7:679–687.
49. Albitar L., Pickett G., Morgan M., Wilken J.A., Maihle N.J., Leslie K.K. (2010) EGFR isoforms and gene regulation in human endometrial cancer cells. Mol Cancer;9:166–179.
50. Waris G., Ahsan H.J. (2006) Reactive oxygen species: role in the development of cancer and various chronic conditions. Carcinogenesis;5:1–8.
51. Gupte A., Mumper R.J. (2009) Elevated copper and oxidative stress in cancer cells as a target for cancer treatment. Cancer Treat Rev;35:32–46.
52. Hileman E.O., Liu J., Albitar M., Keating M.J., Huang P. (2004) Intrinsic oxidative stress in cancer cells: a biochemical basis for therapeutic selectivity. Cancer Chemother Pharmacol;53:209–219.
53. Trachootham D., Alexandre J., Huang P. (2009) Targeting cancer cells by ROS-mediated mechanisms: a radical therapeutic approach? Nat Rev Drug Discov;8:579–591.
54. Kim K.K., Singh R.K., Strongin R.M., Moore R.G., Brard L., Lange T.S. (2011) Organometallic Iron(III)-salophene exerts cytotoxic properties in neuroblastoma cells via MAPK activation and ROS generation. PLoS ONE;6:e19049.
55. Horan T.C., Zompa M.A., Seto C.T., Kim K.K., Moore R.G., Lange T.S. (2011) Description of the cytotoxic effect of a novel drug abietyl-isothiocyanate on endometrial cancer cell lines. Invest New Drugs; DOI: 10.1007/s10637-011-9728-z.
56. Osone S., Hosoi H., Kuwahara Y., Matsumoto Y., Lehara T., Sugimoto T. (2004) Fenretinide induces sustained-activation of JNK/p38 MAPK and apoptosis in a reactive oxygen species-dependent manner in neuroblastoma cells. Int J Cancer;112: 219–224.
57. Kang Y.H., Lee S.J. (2008) The role of p38 MAPK and JNK in Arsenic trioxide-induced mitochondrial cell death in human cervical cancer cells. J Cell Physiol;217:23–33.

Note

[a]American Cancer Society: Cancer Facts and Figures (2010) http://www.cancer.org.